10.18605/2175-7275/cereus.v15n4p255-267

ARTIGO ORIGINAL

<< Recebido em: 11/09/2023 Aceito em: 13/11/2023. >>

Salinity determination at the paraíba do sul river delta using empirical correlations and the Google Earth engine platform

Determinação da salinidade no delta do rio Paraíba do Sul empregando correlações empíricas e a plataforma Google Earth Engine

Pedro H. Dias de Araújo[1], David de Andrade Costa[2], Simone Vasconcelos da Silva[3], Edna N. Yamasaki[4], Ioannis Kyriakides[5], Antônio J. Silva Neto[6]

RESUMO

O monitoramento da qualidade da água é uma tarefa difícil, e a salinidade é um dos fatores mais relevantes, com implicações na comunidade aquática e no fornecimento de água para a população. A aplicação de correlações empíricas em imagens de satélite para a determinação da salinidade é um recurso que pode ser empregado em regiões estuarinas. O presente estudo aplicou três correlações empíricas, os algoritmos Cilamaya e Cimandiri, e o Índice de Salinidade de Diferença Normalizada em pontos localizados no estuário do rio Paraíba do Sul e em mar aberto, com o objetivo de testar a eficácia dos métodos aplicados. Ao se analisar todos os pontos, o algoritmo Cimandiri apresentou melhor correlação em pontos com maior salinidade, e o Cilamaya apresentou melhor correlação em pontos localizadas no interior do estuário. Pode-se concluir que os algoritmos podem ser utilizados para determinação de salinidade, mas estudos recentes indicam que a aplicação de técnicas de machine learning podem obter resultados melhores para o presente propósito.

Palavras-chave: Salinidade, Estuário, Imagens de Satélite, Correlações Empíricas

ABSTRACT

Salinity is one of the most relevant factors when monitoring water quality because of its impact in both aquatic environment and water supply destined to human consumption. Empirical correlations applied to satellite images can be utilized to determine salinity in estuarine areas. The present study used three empirical correlations, Cilamaya and Cimandiri algorithms and the Normalized Difference Salinity Index at points located in the Paraíba do Sul River estuary and at open sea, with the purpose of testing the efficacy of the applied methods. The results indicated that the Cimandiri algorithm showed better correlations at points with higher salinity, and the Cilamaya algorithm presented better correlations at points located at areas within the estuary. It was concluded that these algorithms can be used for salinity determination. Although these algorithms can be used for salinity determination, recent studies show that application of machine learning techniques can obtain better results for this purpose.

Keywords: Salinity, Estuary, Satellite Imagery, Empirical Correlations

[1] **Mestre em Engenharia dos Materiais. Instituto Federal Fluminense, Campus Campos Centro.**

E-mail: pedro.araujo@iff.edu.br

ORCID: https://orcid.org/0009-0000-6394-236X

[2] **Doutor em Recursos Hídricos, Instituto Federal Fluminense, Campus Avançado São João da Barra.**

Email: david.costa@iff.edu.br

ORCID:https://orcid.org/0000-0003-1814-5892

[3]**Pós-Doutorado em Engenharia/Modelagem Computacional. Instituto Federal Fluminense, Campus Campos Centro.**

Email: simonevs@iff.edu.br

ORCID: https://orcid.org/0000-0002-5994-6840

[4]**Ph.D em Biofísica, Universidade de Nicosia**

Email: yamasaki.e@unic.ac.cy

ORCID: https://orcid.org/0000-0002-5212-8079

[5] **Ph.D em Engenharia Elétrica, Universidade de Nicosia.**

Email: kyriakides.i@unic.ac.cy

ORCID: https://orcid.org/0000-0002-3580-088X

[6] **Ph.D em Engenharia Mecânica, Universidade do Estado do Rio de Janeiro, Instituto Politécnico.**

Email: ajsneto@iprj.uerj.br

ORCID: https://orcid.org/0000-0002-9616-6093

1. INTRODUCTION

The term “delta” was coined by Herodotus, around 450 BC, while observing the similarity between the shape of the mouth of the Nile River and the pattern of sediment deposition with the Greek letter delta, “Δ”. Deltas are subaerial and submarine coastal sediment accumulations formed near river mouths, from the hydrodynamic interaction of the river currents carrying sediments to its mouth and the sea front, acting through waves, currents and tidal changes (GALLOWAY, 1975).

The city of São João da Barra is located at the mouth of the Paraíba do Sul River (PSR). Over the years, remodeling along its course resulted in decreased water flow at the mouth of the river, and intrusion of sea water into the river channel have been shown to affect the quality of water destined for human consumption. Whenever salinity levels exceed defined thresholds, water abstraction from the PSR is stopped, a fact that has recently become very frequent (CEDAE, 2022; FOLHA 1, 2021).

The outlet of the PSR is shaped like a delta, and the islands formed by the deposition of sediments divide the cities of São João da Barra, called the southern flank, and São Francisco do Itabapoana, the northern flank. The two mouths in the PSR delta can be considered estuarine environments, firstly due to the physicochemical characteristics of their waters (BARROSO *et al*., 2019; NUNES *et al*., 2022) and secondly, due to the local hydrodynamics, primarily dependent on the flow of the PSR and the waves and tides of the Atlantic Ocean. The PSR originates in the State of São Paulo and supplies water to parts of the states of São Paulo, Minas Gerais and Rio de Janeiro, altogether reaching close to 25.7 million people (CEIVAP, 2022). The consequences of the use and transposition of PSR waters are a growing concern, especially for the conservation of an instream flow.

Estuaries can be classified according to their geometry, geomorphology, hydrodynamics, salinity, and tide. An estuary is the terminal zone of a river that flows into a tidal sea, thus constituting a transitional body of water between the river and the sea, and whose salinity varies temporally and spatially within it. The sea water is diluted with fresh water from the respective river drainage basin, being responsible for the salinity gradients that condition the typical estuarine circulation types (POTTER *et al*., 2010). If the river discharge decreases, the marine influence increases, increasing the estuarine area or the salinity in the inner region of the estuary. If river discharge increases, the mixture moves towards the ocean (LOITZENBAUER and BULHÕES, 2011).

Salinity measures the concentration of dissolved salts in water, and is commonly expressed in parts per thousand (ppt). The salinity gradients along the estuary can vary from values close to those of the river's fresh water, called limnetic, with salinity lower than 0.5 ppt to regions with salinity greater than 40.0 ppt. According to salinity values, estuary regions are classified in oligohaline regions with salinity values between 0.5 to 5.0 ppt, mesohaline regions between 5.0 to 18.0 ppt, polyhaline regions varying between 18.0 to 30.0 ppt, euhaline regions between 30.0 and 40.0 ppt, and finally hyperhaline regions with salinity greater than 40.0 ppt (MITSCH and GOSSELINK, 2007).

In the PSR estuary, during high tide, the salinity gradient increased due to a greater inflow of salt water. However, even at low tide and with low river flow, high salinity was observed within the last 1,400 meters of the river bed (BARROSO, 2019). There is no strong correlation between other climatic factors and salinity, with the PSR outflow being the main determinant for the salinity of the estuary.

Results obtained by NUNES *et al*. (2022) analyzing the physicochemical characteristics of water samples supported these findings, and river flows of less than 360 m3/s result in salinity greater than 0.5 ppt in stretches of 2 km from the coast.

Monitoring saline intrusion through physicochemical analyses can be costly, and while they provide more accurate results about the concentration of salts in water, the spatial and temporal distribution of such data are generally limited and cannot be extrapolated to long-term projections or over large areas. Alternatively, remote sensing has proven to be an effective technique for analyzing water quality parameters (BAYATI and YAZDI, 2021).

The first attempt to obtain indirect values for salinity by processing satellite images was carried out by KHORRAN (1982). However, at that time, the correlation between reflectance and salinity values were low, thereby invalidating the use of the technique for the specific purpose. The best correlations between the reflectance of the studied bands have been obtained recently, with the application of machine learning techniques (HASSAN and WOO, 2021).

SAKAI *et al*. (2021) monitored saline intrusion in the Ayeyarwady Delta, Myanmar. The study obtained images from Sentinel-2 satellite with high spatial (10m) and temporal (10 days) resolutions, and the reflectance of the visible bands correlated with the electrical conductivity, which is influenced by the concentration of dissolved salts. When fresh water from the river mixed with salt water from the sea, the suspended particles tended to flocculate and settle, so that the less turbid water had higher salinity. In this study, the best models obtained the highest correlation with the reflectance of the green band (R^2 of 0.776).

BAYATI and YAZDI (2021) investigated the effectiveness of different machine learning techniques (artificial neural networks, multiple linear regression, and fuzzy logic) in obtaining salinity values through the processing of Sentinel-2 and Landsat-8 satellite images in the hypersaline Lake Urmia. The results of this study indicated that artificial neural networks obtained the best correlation between salinity and reflectance of the blue, green, and red bands (R^2 0.94).

MUKHTAR *et al*. (2021) applied several algorithms to estimate salinity (Cimandiri, Wouthuyzen and Cilamaya algorithms) and the concentration of suspended solids (Parwati, Budhiman and Lestari algorithms) from images obtained with Landsat-8 and Sentinel-2 using Google Earth Engine. The results obtained by the analysis demonstrated the effectiveness of the algorithms to detect the properties studied, in particular the Cilamaya algorithm with Sentinel 2 images for salinity detection (R^2 of 0.53) and the Budhiman algorithm for obtaining total solids suspended (R^2 of 0.52).

The use of image processing through remote sensing provides a more extensive set of data than those obtained in the field, and with substantially better spatial and temporal resolutions. Examples of satellites used for this purpose are: Landsat, Sentinel, MODIS, MERIS and VIIRS (HASSAN and WOO, 2021).

Landsat-8 has a spatial resolution of 30 meters and a temporal resolution of 16 days. Its images can detect changes in large water bodies in small time intervals. Recently, NGUYEN *et al*. (2018), SAKAI *et al*. (2021), BAYATI and YASDI (2021) and MUKTHAR *et al*. (2021) used successfully Landsat-8 image processing to indirectly measure salinity in water bodies by applying empirical correlations.

In this context, this work aims to test the applicability of the Cimandiri (SUPRIATNA *et al*., 2016) and Cilamaya (KAFFA *et al*., 2020) algorithms and the Normalized Difference Salinity Index, or NDSI (KHAIER, 2003), to indirectly determine the salinity levels through the processing of Landsat 8 satellite images in the PSR estuary region, using the Google Earth Engine platform.

2. MATERIALS AND METHODS

The selected study area is the estuary of the Paraiba do Sul River, located in between the municipalities of São João da Barra and São Francisco do Itabapoana in the northern region of the state of Rio de Janeiro, Brazil. The effectiveness of the methods applied in this

study were compared to actual salinity values, from *in situ* analyses performed by INEA (INEA, 2015).

The algorithms used have been shown to provide better correlations in regions of high salinity (SUPRIATNA *et al*., 2016, KAFFA *et al*., 2020, KHAIER, 2003), so, three different locations in the PSR estuary were chosen: a region subject to intense tidal action (p1, p1 and p3), which may have greater or lesser salinity depending on the river flow and tidal variation, and a control point in the open sea (p0), considering the sea salinity of approximately 35 ppt. Totaling 4 points studied, with the following coordinates: p0 (-21.5783944, -40.7435841), p1 (-21.61808289, -41.01599626), p2 (-21.61829521, -41.02379314) and p3 (-21.61830202, -41.03211833), WGS1984 datum, which are shown highlighted in Fig. 1, with the exception of p0, located at open sea.

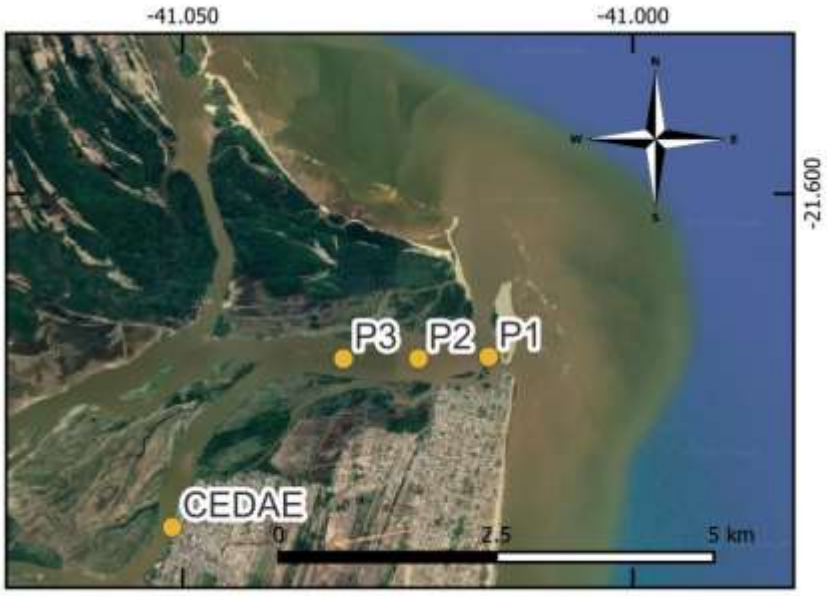

Figure 1- Location of points p1, p2 and p3 (Source: INEA, 2015).

Satellite images were obtained from the Landsat-8 Level-2, Collection-2, Tier-2 collection), containing atmospherically corrected surface reflectance and surface temperature data derived from data produced by OLI/TIRS sensors. The images contain 7 bands, namely, ultra-blue, blue, green, red, near infrared, short infrared 1 (SWIRI) and short infrared 2 (SWIRII), each representing a wavelength range of the radiation captured by the satellite.

Salts dissolved in water, depending on the chemical species, reflect light at preferred wavelengths (HANLEY *et al*., 2014). Correlation between the bands obtained with the

Cimandiri (SUPRIATNA *et al*., 2016), Cilamaya (KAFFA *et al*., 2020) and NDSI (KHAIER, 2003) algorithms allow for indirect values of salinity. These equations were applied at the location points studied in the present work, shown in Fig.1, are presented in Table 1.

The implementation of the algorithms and extraction of the analyzed points were carried out using the Google Earth Engine tool, with implementation in JavaScript. The coordinates of the points were loaded into the code compiler, the images were imported with the image collection function, the analyzed period was delimited by the data filter function, and the correlation equations between the bands were implemented in the code. Salinity data were extracted using the export function, where salinity values are tabulated according to the date when the satellite passed over the area under analysis. Image metadata was used to remove data influenced by clouds or shadows

Table 1- Algorithms for salinity used in this work.

Algorithm	**Equation**	**Year**
Cimandiri	29.983+(165.047*Blue)-(260.227*Green)+ (2.609*Red)	2016
Cilamaya	139.556970+(86.21318*lnBlue)- (24.62518*lnRed) ln= natural logarithm	2019
Normalized Difference Salinity Index	(SWIRI−SWIRII)/(SWIRI+SWIRII)	2003

Pearson's correlation coefficient (R), defined in Eq. 1, was used to evaluate the applicability and effectiveness of the methods for obtaining indirect salinity measurements.

$$R = \frac{\sum(x-\bar{x})(y-\bar{y})}{\sqrt{\sum(x-\bar{x})^2 \sum(y-\bar{y})^2}} \quad (1)$$

where, y is the dependent or resulting variable, and x the independent or causal factor variable and $\bar{y}$ and $\bar{x}$, the average values, respectively. Table 2 presents the correlation conditions applied in the present work. Positive values represent directly proportional correlation and negative values represent inversely proportional correlation.

Table 2 – Correlation Conditions (MUKHTAR *et al*., 2021).

Correlation Coefficient	**Correlation Condition**
0	No correlation

0 – 0.25	Weak correlation
0.25 – 0.5	Enough Correlation
0.5 – 0.75	Strong correlation
0.75 – 0.99	Very strong correlation
1	Perfect correlation

The salinity results obtained by the algorithms were compared with data measured *in situ* in INEA campaigns to monitor saline intrusion in the PSR estuary, in one of the biggest water crises in the basin between 2014 and 2015, and with salinity in the open sea at one point.

3. RESULTS

Table 3 – Salinity values obtained with the chosen algorithms.

Dates	Points	Sal. Ref.	Cimandiri	Cilamaya	NDSI
02/Nov/2014	p0	35.000	22.737	13.335	0.040
	p1	33.850	6.370	21.718	0.068
	p2	24.700	7.050	22.624	0.066
	p3	15.030	6.900	22.717	0.063
04/Dez/2014	p0	35.000	25.668	53.483	0.084
	p1	34.230	7.670	3.445	0.156
	p2	12.110	8.190	3.199	0.176
	p3	4.760	8.190	9.709	0.166
21/Jan/2015	p0	35.000	25.857	83.311	0.209
	p1	29.880	12.135	29.118	0.135
	p2	24.490	12.434	40.221	0.173
	p3	19.050	10.885	40,007	0.154
Pearson (R)			**0.55**	**0.39**	**-0.25**

After carrying out the image processing steps, using Google Earth Engine, a spreadsheet was created with the salinity values for each algorithm, with one salinity measurement per day, every 16 days (temporal resolution of Landsat-8). The dates that coincided with the *in situ* physicochemical analyzes (INEA, 2015) were chosen and are presented in Table 3.

While the Cimandiri and Cilamaya algorithms showed a positive correlation between the direct (*in situ*) and indirect salinity measurements, NDSI was the only method to present a negative correlation, which implies an inversely proportional relationship. The Cimandiri algorithm showed the highest correlation.

It can be noted that there was little variation in the values for the methods within the same date, which implies a low correlation, since the values observed for the *in situ*

measurements vary increasingly as one enters the river; p1 is closer to the mouth (higher salinity) and p3 further away from the mouth towards the river (lower salinity). Such behavior can be noticed in the three dates studied.

Figure 2 shows the graphs of the salinity profile obtained by the studied methods and by the *in situ* measurements for the analyzed points. The points were calculated by applying the affine function obtained by each linear regression (Fig. 4). The twelve points represent p0, p1, p2 and p3 in the three analyzed days. It can be noted that the tendency for salinity to decrease as one moves away from the mouth towards the river is evidenced by the slope of the curve between p0 and p3.

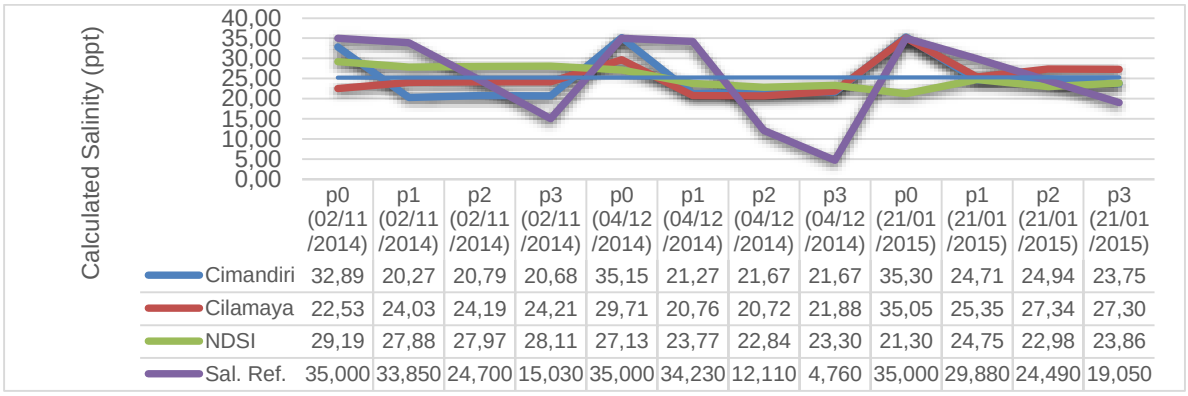

	p0 (02/11 /2014)	p1 (02/11 /2014)	p2 (02/11 /2014)	p3 (02/11 /2014)	p0 (04/12 /2014)	p1 (04/12 /2014)	p2 (04/12 /2014)	p3 (04/12 /2014)	p0 (21/01 /2015)	p1 (21/01 /2015)	p2 (21/01 /2015)	p3 (21/01 /2015)
Cimandiri	32,89	20,27	20,79	20,68	35,15	21,27	21,67	21,67	35,30	24,71	24,94	23,75
Cilamaya	22,53	24,03	24,19	24,21	29,71	20,76	20,72	21,88	35,05	25,35	27,34	27,30
NDSI	29,19	27,88	27,97	28,11	27,13	23,77	22,84	23,30	21,30	24,75	22,98	23,86
Sal. Ref.	35,000	33,850	24,700	15,030	35,000	34,230	12,110	4,760	35,000	29,880	24,490	19,050

Figure 2 – Calculated salinity profile graphs.

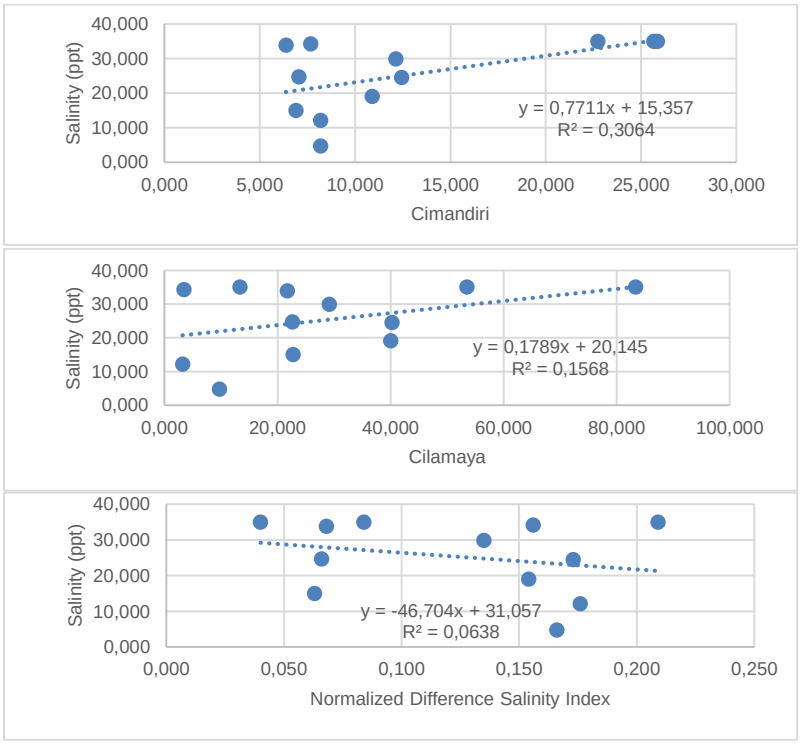

Figure 3 – Linear regression graphs obtained with the methods used.

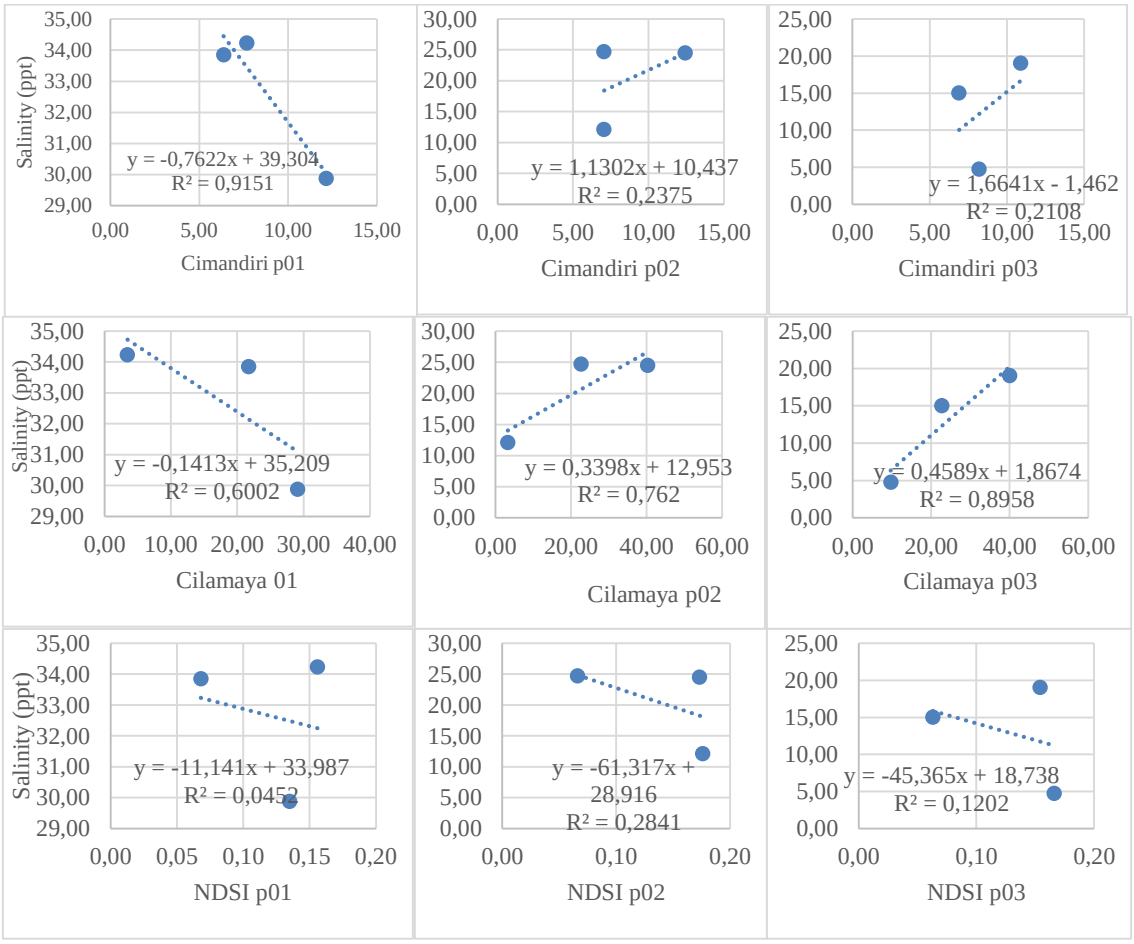

Figure 4 – Linear regression graphs obtained at points p1, p2 and p3.

Figure 3 shows the three linear regression graphs obtained for the methods applied to all points studied here. The R^2 values obtained for the Cimandiri, Cilamaya and NDSI algorithms were 0.3064, 0.1568 and 0.06318, respectively.

Figure 4 shows the regressions for each point. The correlation presented by NDSI has the same behavior as that observed in Fig. 4: weak correlation. Analyzing only points p02 and p03, the Cilamaya algorithm showed better correlations (R^2), 0.762 and 0.8958, respectively. The Cimandiri showed the highest correlation at the p0 points, that is, in regions of high salinity, in the open sea.

4. DISCUSSION

Several previous studies have successfully applied the algorithms studied in the present work (MUKTHAR *et al.*, 2021; TUNJUNG *et al.*, 2021; KAFFA *et al.*, 2020; SUPRIATNA *et al.*, 2016; KHAIER, 2003), which justifies the use of such techniques for image processing and obtaining salinity values indirectly.

In the mentioned previous works better correlations values were obtained than those present in this work. Some factors may have contributed to the dispersion of data obtained here.

The small number of points available for comparison and the collection on different days contribute to the heterogeneity of the samples. The region is highly susceptible to the action of the tidal field, consequently in the same day the salinity changes at the same point due to estuarine dynamics (BARROSO *et al*., 2019). Besides it was not possible to synchronize the satellite pass with the data measured *in situ*. A more accurate data collection in relation to the satellite passage and the effects of the tide can support a more extensive study of the correlation of the studied techniques with the salinity *in situ*.

Another possibility would be to process images from Sentinel-2 satellite, as it has a temporal resolution of 6 days and a spatial resolution of 10 meters (EARTH ENGINE CATALOG, 2022), which would facilitate the synchronization of sample collection with the passage of the satellite.

In a systematic literature review carried out by HASSAN and WOO (2021), on the application of machine learning techniques to indirectly obtain salinity, 113 works were found that used techniques such as artificial neural networks, support vector machines, random forest, decision trees, multilayer perceptron network, cubic regression and Gaussian regression for monitoring water quality, including salinity. Several works obtained indicative values of correlation, and the high number of recent works found in the review demonstrates the high interest in such techniques for the purpose of the present work.

5. FINAL CONSIDERATIONS

Three methods for indirectly obtaining salinity (empirical algorithms Cimandiri, Cilamaya and NDSI) were applied at four points in the region close to the estuary of the Paraíba do Sul River on three different dates. The salinity values obtained were compared with data provided by INEA in a saline intrusion monitoring in the study region.

The effectiveness of the methods for this purpose was evaluated using R and R^2 coefficients. The Cimandiri algorithm showed the highest correlation among the applied methods, with an R of 0.55. However, this value is too low to conclude that there is data correlation, that is, with the results obtained, it cannot be concluded that the Cimandiri algorithm is appropriate or not for studying salinity in the PSR estuary.

For this purpose, it is suggested for future work: a collection of a greater number of samples on days that coincide with the passage of the satellite in question; the use of images from satellites with higher space-time resolution, Sentinel-2, for example; and the use of machine learning techniques to study the most appropriate band ratio for the region in question.

5. ACKNOWLEDGEMENTS

The authors acknowledge the financial support provided by the following Brazilian agencies: FAPERJ, Carlos Chagas Filho Foundation for Research Support of the State of Rio de Janeiro; CNPq, National Council for Scientific and Technological Development; and CAPES, Coordination for the Improvement of Higher Education Personnel (Finance Code 001). Acknowledgements are also due to the European Erasmus Program, through the University of Nicosia Erasmus Office.

REFERENCES

BARROSO, G. C; SILVA, L. B. C.; OLIVEIRA, V. P. S. Analysis of the Correlation Between Salinity and Environmental Variables in the Estuary of the Paraíba do Sul River – Brazil. **As Ciências do Mar em todos os seus aspectos**, Atena Editora, 1 ed, p. 103-117, 2019.

BAYATI, M.; YAZDI, M. D. Mapping the spatiotemporal variability of salinity in the hypersaline Lake Urmia using Sentinel-2 and Landsat-8 imagery. **Journal of Hidrology**, n 595, 126032, fev 2021.

CEDAE, 2022. Disponível em: <https://cedae.com.br/Noticias/detalhe/intrusao-salina-causa-instabilidade-no-abastecimento-de-sao-joao-da-barra/id/2347> acessado em 04/09/2022.

CEIVAP, 2022. Disponível em: <ceivap.org.br> acessado em 02/09/2022.

EARTH ENGINE CATALOG, 2022, Disponível em: <https://developers.google.com/earth-engine/datasets/catalog/LANDSAT_LC08_C02_T2_L2> acessado em 04/09/2022.

FOLHA, 2021. Disponível em: <https://www.folha1.com.br/_conteudo/2021/07/na_foz/1274128-intrusao-salina-provoca-reducao-no-abastecimento-de-agua-em-sjb> acessado em 04/09/2022.

GALLOWAY, W. E. **Process framework for describing the morphologic and stratigraphic evolution of delta depositional systems**. Deltas: Models for Exploration, BROUSSARD M. L, Houston Geological Society, Houston, p. 87–98, 1975.

HANLEY, J.; DALTON III, J. B.; CHEVRIER, V. F.; JAMIESON, C. S.; BARROWS, R. S. Reflectance spectra of hydrated chlorine salts: The effect of temperature with implications for Europa. **Journal of Geophysical Research: Planets**, n. 119, p. 2370-2377, 2014.

HASSAN, N.; WOO, C. S. Machine Learning Application in Water Quality Using Satellite Data. **IOP Conf. Series: Earth and Environmental Science,** n. 842, 012018, 2021.

INEA **Water Quality Monitoring, Rivers Paraíba and Guandu**. Diretoria de Gestão das Águas e do Território, Gerência de Avaliação de Qualidade das Águas, 2015.

KAFFA, S.; SUPRIATNA; DAMAYANTI, A. Cilamaya estuary zonation based on sea surface salinity with 2 Sentinel-2A satellite imagery. **IOP Conf. Series: Earth and Environmental Science,** n. 481, 012071, 2020.

KHAIER, F. A **Soil Salinity Detection Using Satellite Remote Sensing**. Dissertação de Mestrado, International Institute for Geo-Information Science and Earth Observation Enschede, The Netherlands, 2003. Disponível em: <https://webapps.itc.utwente.nl/librarywww/papers_2003/msc/wrem/khaier.pdf>

KHORRAN, S. Remote Sensing of Salinity in the San Francisco Bay Delta. **Remote Sensing of Environment**, n. 12, p 15-22, Elsevier, 1982.

LOITZENBAUER, E. A; BULHÕES, C. A. Dinâmica da salinidade como uma ferramenta para a gestão integrada de recursos hídricos na zona costeira: uma aplicação à realidade brasileira. **Revista da Gestão Costeira Integrada**, v. 11, n. 2, p.233-245, 2011.

MITSCH, W. J.; GOSSELINK, J. G. **Wetlands**. 4° ed, John Wiley and Sons, 2007.

MUKHTAR, M. K.; SUPRIATNA, MANESSA, M. D. M. The validation of water quality parameter algorithm using Landsat 8 and Sentinel-2 image in Palabuhanratu Bay **IOP Conf. Series: Earth and Environmental Science,** n. 846, 2021.

NGUYEN, P. T. B.; KOEDSIN, W.; MCNEIL, D.; Van, T. P. D. Remote sensing techniques to predict salinity intrusion: application for a data-poor area of the coastal Mekong Delta, Vietnam. **International Journal of Remote Sensing**, n. 39, p. 6676–6691, 2018.

NUNES, C. R. O.; PRÉ, H. L. S.; SILVA, K. C; NETO, P. B.; OLIVEIRA, V. P. S.; ARAÚJO, T. M. R. Ionic Characterization and salinity evaluation in the Paraíba do Sul River estuary, southeast, Brazil, between 2018 and 2019. **Regional Studies in Marine Science**, n. 55, 102507, Elsevier, 2022.

POTTER, I. C., CHUWEN, B. M., HOEKSEMA, S. D., ELLIOT, M. The concept of an estuary: A definition that incorporates systems which can become closed to the ocean and hypersaline Estuarine. **Coastal and Shelf Science**, n. 87, p. 497-500, 2010.

SAKAI, T.; OMORI, K.; OO, A. N.; ZAW, Y. N. Monitoring saline intrusion in the Ayeyarwady Delta, Myanmar, using data from the Sentinel-2 satellite mission. **Paddy and Water Environment**, Springer, 2021.

SUPRIATNA, I.; SUPRIATNA, J.; KOETSOER, R. H.; TAKARINA, N. D. Algorithm Model for the Determination of Cimandiri Estuarine Boundary using Remote Sensing **AIP Conference Proceedings**, n. 1729, 020079, 2016.

TUNJUNG, D. M.; SUPRIATNA, S.; SHIDIG, I. P. A.; MANESSA, M. D. M. Estuary zone based on sea level salinity in Ciletuh Bay, West Java. **IOP Conf. Series: Earth and Environmental Science**, n. 623, 2021.